JOURNAL OF PETROLEUM GEOMECHANICS
(JPG)

Original article

Treatment of relative permeability term in two-phase flow problems in porous media

Ehsan Taheri[1*], Seyed Ali Ghoreishian Amiri [2]

1- Department of Rock Mechanics, Tarbiat Modares University, Tehran, Iran
2- PoreLab, Department of Civil and Environmental Eng., Norwegian University of Science and Technology (NTNU), Trondheim, Norway.

Received: 18 August 2022; Accepted: 17 October 2022

DOI: 10.22107/jpg.2022.362663.1179

Keywords

Two-phase flow,
Porous media,
Pressure-based solution,
Relative permeability

Abstract

This paper presents a control volume finite element model (CVFEM) to simulate simultaneous flow of two immiscible fluids in non-deformable porous media. The method is fully conservative at the local and global level. It keeps the data structure of the common finite element method (FEM). A pressure-based formulation is presented in this paper. The proper choice of primary unknown variables is a critical step in developing an efficient solution of the multiphase subsurface flow problems. Pressure-based models are one of the common choices to this end. This type of models consists of strong nonlinear terms and encounters convergence difficulties when the Jacobian matrix are poorly approximated. The most severe problem is related to the relative permeability term that appears as a function of volume fraction (or degree of saturation) of the wetting phase. Since water saturation is not a primary unknown variable, the relative permeability terms become a function of two primary unknowns, i.e. wetting and non-wetting pressures, together. A fully implicit first order accurate finite difference scheme is employed for temporal discretization of the equations. A full Newton method with exact Jacobian is considered in this work, and a rapid convergence has been achieved. The model is used to simulating a five-spot problem in a block heterogenous porous medium.

1. Introduction

Numerical simulation of simultaneous flow of two or three immiscible fluids in geological porous media is of great interest in many engineering disciplines. Areas of applications include, among the others, natural gas and oil recovery, geothermal energy utilization, underground waste repositories, geological sequestration of CO_2, and underground gas storage. Numerical modelling of such problems consists of a system of highly nonlinear and coupled partial differential equations. As a consequence, in addition to the requirement of extensive computational resources, they cannot be usually solved satisfactorily using standard numerical techniques. Thus, a number of almost exclusive numerical techniques have been suggested, e.g. [1-4], for the treatment of numerical problems regarding instabilities and truncation errors associated with various nonlinearities involved in these problems.

In general, the numerical schemes adopted for modeling multiphase flow in porous media consist of spatial discretization of mass conservation equations; their temporal discretization; and an iterative solver, such as newton iteration, to solve the obtained system of nonlinear algebraic equations. The studies of modeling multiphase flow through porous media, e.g. [5-8], identified that the choice of primary variables for newton iteration has a significant impact on computational performance of the model.

One of the common selections of primary variables is to select the fluid phases pressure, which known as pressure-based formulation. In

* Corresponding Author: E-mail address: e_taheri@modares.ac.ir

this approach, the governing equations are written in terms of pressure in each phase through a straightforward substitution of the Darcy's equation into the mass balance equation of each phase. This approach is adopted by a number of researchers, e.g. [9-11], and reasonable results are reported. This approach works well when the wetting phase effectively exists in the medium.

In this paper, we practice a CVFE model to simulate simultaneous flow of two immiscible flow in porous materials, with a full Newton solver that can handle the severe nonlinearity associated with relative permeability variation.

2. Governing equations

The system of concern is a an isothermal rigid porous medium saturated with two immiscible and incompressible fluids (wetting, w, and non-wetting, n, phases). The multiphase system is described using the assumption of superposition; i.e. any spatial point, $\mathbf{x}$, in the solution domain, is simultaneously occupied by material points of all phases, $\mathbf{X}_\alpha$, while their motions are described independently.

The flow of each phase is described using its mass conservation equation:

$$\rho_\alpha \frac{\partial n_\alpha}{\partial t} + \nabla^T (n_\alpha \rho_\alpha \bar{\mathbf{v}}_\alpha) = 0, \quad \alpha = w, n \tag{1}$$

and the generalized Darcy's law:

$$n_\alpha \bar{\mathbf{v}}_\alpha = \mathbf{q}_\alpha = \frac{k_{r\alpha}\mathbf{K}}{\mu_\alpha}\left[\rho_\alpha \mathbf{g} - \nabla p_\alpha\right] \tag{2}$$

where n_α denotes the volume fraction of phase α, ρ stands density, $\bar{\mathbf{v}}_\alpha$ denotes the relative velocity of phase α with respect to the solid skeleton, **g** is the gravitational acceleration vector, $\mathbf{q}_\alpha$ is the flux of phase α, P stands for pressure, **K** is the absolute permeability tensor, μ denotes dynamic viscosity and k_r is the relative permeability that is related to the volume fraction of the wetting phase, n_w:

$$k_{rw} = \mathsf{A}\ (n_w) \tag{3}$$

$$k_{rn} = \mathsf{G}(n_w) \tag{4}$$

Fluids interaction can be considered using empirical correlations relating the capillary pressure,

$$p_c = p_n - p_w:$$

$$n_w = \mathsf{F}\ (p_c) \tag{5}$$

Indeed, the following constraint must be satisfied:

$$n_w + n_n = n \tag{6}$$

where n denotes porosity.

Differentiating Eqs. (5) and (6) results:

$$dn_w = \frac{dn_w}{dp_c} dp_c = n'_w \left(dp_n - dp_w\right) \tag{7}$$

$$dn_n = -dn_w \tag{8}$$

Substituting Eqs. (7) and (8) into Eq. (1) will result in:

$$\left(-n'_w \rho_w\right)\frac{\partial p_w}{\partial t} + \left(n'_w \rho_w\right)\frac{\partial p_n}{\partial t} + \nabla^T\left(\rho_w \mathbf{q}_w\right) = 0 \tag{9}$$

$$\left(-n'_w \rho_o\right)\frac{\partial p_n}{\partial t} + \left(n'_w \rho_o\right)\frac{\partial p_w}{\partial t} + \nabla^T\left(\rho_n \mathbf{q}_n\right) = 0 \tag{10}$$

2.1. Initial and boundary conditions

Equations (9) and (10) represent a system of two highly nonlinear and strongly coupled partial differential equations defined on a domain **Ω** bounded by Γ. The fluids pressure, P_w and P_n, are selected as the primary unknown variables. In order to complete the system of equations, the initial and boundary conditions associated with the primary variables should be defined. The initial condition should specify the fluid pressures at time t=0:

$$p_\alpha = p_\alpha^0, \quad \text{at } t = 0, \text{ on } \Omega \text{ and } \Gamma \tag{11}$$

Dirichlet boundary conditions are imposed as prescribed values of the primary variables on the boundaries:

$$p_\alpha = \bar{p}_\alpha, \quad \text{on } \Gamma_{p_\alpha} \tag{12}$$

and Neumann boundary conditions are imposed as prescribed fluxes:

$$\bar{q}_\alpha = \left\{\rho_\alpha \frac{k_{r\alpha}\mathbf{K}}{\mu_\alpha}\left[\rho_\alpha \mathbf{g} - \nabla p_\alpha\right]\right\}^T .\mathbf{n}, \quad \text{on } \Gamma_{q_\alpha} \tag{13}$$

where $\bar{q}_\alpha$ is the imposed mass flux of phase α, **n** denotes the unit outward normal vector to the boundary:

$$\mathbf{n} = \left\{n_x \quad n_y \quad n_z\right\}^T \tag{14}$$

The conditions $\Gamma_{p_w} \cup \Gamma_{q_w} = \Gamma$, $\Gamma_{p_n} \cup \Gamma_{q_n} = \Gamma$ should

hold on the complementary parts of the boundary.

3. Numerical solution

Hexahedral elements are employed in this work to discretize the physical domain. The field variables (p_w, p_n) are interpolated in terms of their corresponding nodal values $(\mathbf{p}_w, \mathbf{p}_n)$:

$$p_w = \mathbf{N}\mathbf{p}_w, \quad p_n = \mathbf{N}\mathbf{p}_n \tag{15}$$

where $\mathbf{N}$ represents the standard finite element shape functions for hexahedral elements.

3.1. Mass balance equations - CVFEM

In order to derive the CVFE formulation of the governing equations (9) and (10) through a procedure similar to the FEM, the following weighting functions, $\mathbf{W}$, are considered:

$$W_i = H(\xi.\xi_i).H(\eta.\eta_i).H(\zeta.\zeta_i) \tag{16}$$

where ξ, η, ζ are the standard natural (local) coordination system of the element, the subscript i denotes the element nodes, and H is the Heaviside function:

$$H(x) = \begin{cases} 1 & x \geq 0 \\ 0 & x < 0 \end{cases} \tag{17}$$

This weighting function implicitly divides the element into subdomains belonging to each node. This is known as the *subdomain collection technique*. Fig. 1-a shows the subdomain corresponding to node i. As shown, there are internal surfaces (abcd, abef, bcfg), namely internal boundaries (Γ_{int}), that separate this subdomain from the rest of the element.

The fundamental properties of the Heaviside function include [12]:

$$\int_{\Omega_e} \mathbf{W}^T \nabla^T \mathrm{F}\, d\Omega = \int_{\Omega_s} [\mathbf{1}]^T \nabla^T \mathrm{F}\, d\Omega = \int_{\Gamma_s} [\mathbf{1}]^T \mathrm{F}^T.\mathbf{n}\, d\Gamma \equiv \int_{\Gamma_e} \mathbf{W}^T \mathrm{F}^T.\mathbf{n}\, d\Gamma + \int_{\Gamma_{\text{int}}} \mathbf{W}^T \mathrm{F}^T.\mathbf{n}\, d\Gamma \tag{18}$$

where Ω_e and Ω_s are the domain of the element and the subdomain, respectively, that are bounded by Γ_e and Γ_s, and F denotes a smooth vector field.

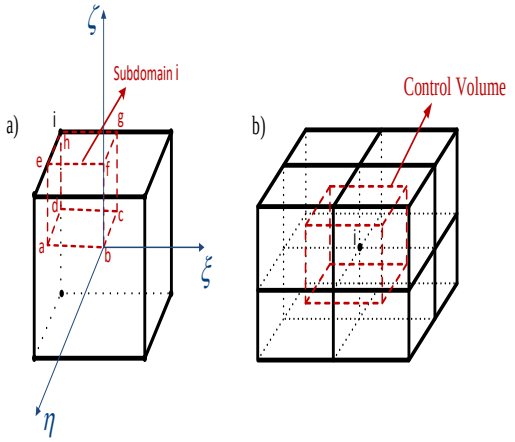

Fig. 1. Schematic representation of subdomain (a); and control volume (b) around node i

Considering equation (18), the weighted residual formulation of equations (9) and (10) over Ω_e, and equation (13) over Γ_e, can be written as:

$$\int_{\Omega_e} \mathbf{W}^T \left(-\rho_w n'_w\right) \frac{\partial p_w}{\partial t} d\Omega + \int_{\Omega_e} \mathbf{W}^T \rho_w n'_w \frac{\partial p_n}{\partial t} d\Omega + \int_{\Gamma_e} \mathbf{W}^T \mathbf{q}_w{}^T.\mathbf{n} d\Gamma + \int_{\Gamma_{\text{int}}} \mathbf{W}^T \mathbf{q}_w{}^T.\mathbf{n} d\Gamma + \int_{\Gamma_e} \mathbf{W}^T \left[\bar{q}_w - \left\{ \rho_w \frac{k_{rw}\mathbf{K}}{\mu_w} \left[\rho_w \mathbf{g} - \nabla p_w\right] \right\}^T .\mathbf{n} \right] d\Gamma = 0 \tag{19}$$

$$\int_{\Omega_e} \mathbf{W}^T \left(-\rho_n n'_w\right) \frac{\partial p_n}{\partial t} d\Omega + \int_{\Omega_e} \mathbf{W}^T \rho_n n'_w \frac{\partial p_w}{\partial t} d\Omega + \int_{\Gamma_e} \mathbf{W}^T \mathbf{q}_n{}^T.\mathbf{n} d\Gamma + \int_{\Gamma_{\text{int}}} \mathbf{W}^T \mathbf{q}_n{}^T.\mathbf{n} d\Gamma + \int_{\Gamma_e} \mathbf{W}^T \left[\bar{q}_n - \left\{ \rho_n \frac{k_{rn}\mathbf{K}}{\mu_n} \left[\rho_n \mathbf{g} - \nabla p_n\right] \right\}^T .\mathbf{n} \right] d\Gamma = 0 \tag{20}$$

As it can be seen, the internal boundaries appeared in the integral form of the partial differential equations. This is the main difference of the CVFE formulation comparing with the FEM.

Using the interpolatory representation of the field variables (equation (15)), the discretized form of the mass balance equations can be written as:

$$\mathbf{P}_{ww}\frac{\partial \mathbf{p}_w}{\partial t}+\mathbf{C}_{wn}\frac{\partial \mathbf{p}_n}{\partial t}+\mathbf{f}_w^{\text{int}}+\mathbf{f}_w^{\text{ext}}=0 \tag{21}$$

$$\mathbf{C}_{nw}\frac{\partial \mathbf{p}_w}{\partial t}+\mathbf{P}_{nn}\frac{\partial \mathbf{p}_n}{\partial t}+\mathbf{f}_n^{\text{int}}+\mathbf{f}_n^{\text{ext}}=0 \tag{22}$$

where the coefficients are listed below:

$$\mathbf{P}_{ww}=\int_{\Omega_e}\mathbf{W}^T\left(-\rho_w n_w'\right)\mathbf{N}d\Omega \tag{23}$$

$$\mathbf{P}_{nn}=\int_{\Omega_e}\mathbf{W}^T\left(-\rho_n n_w'\right)\mathbf{N}d\Omega \tag{24}$$

$$\mathbf{C}_{wn}=\int_{\Omega_e}\mathbf{W}^T\left(\rho_w n_w'\right)\mathbf{N}d\Omega \tag{25}$$

$$\mathbf{C}_{nw}=\int_{\Omega_e}\mathbf{W}^T\left(\rho_n n_w'\right)\mathbf{N}d\Omega \tag{26}$$

$$\mathbf{f}_w^{\text{int}}=\int_{\Gamma_{\text{int}}}\mathbf{W}^T\mathbf{q}_w{}^T.\mathbf{n}d\Gamma \tag{27}$$

$$\mathbf{f}_n^{\text{int}}=\int_{\Gamma_{\text{int}}}\mathbf{W}^T\mathbf{q}_n{}^T.\mathbf{n}d\Gamma \tag{28}$$

$$\mathbf{f}_w^{\text{ext}}=\int_{\Gamma_{q_w}}\mathbf{W}^T\bar{q}_w d\Gamma \tag{29}$$

$$\mathbf{f}_n^{\text{ext}}=\int_{\Gamma_{q_n}}\mathbf{W}^T\bar{q}_n d\Gamma \tag{30}$$

The final set of the nodal equations can now be constructed using the standard assembling algorithm of the FEM. This will join the subdomains from all adjacent elements and forms a bigger subdomain, namely control volume, around each node (Fig. 1-b). Considering the choice of weighting functions (as shown in equation (16)), all the integrals in equations (21) and (22) will be automatically zero outside of the corresponding control volumes. It means, the mass balance equations are, in fact, satisfied in the control volumes, although they are presented at element level. In addition, the flux terms, which are discontinues between the adjacent elements, are only appeared in surface integral terms on the internal boundaries (as shown in equations (27) and (28)). Consequently, discontinuity of the velocity field between adjacent elements does not affect the local conservative characteristic of the calculations over the control volumes. Indeed, construction of the control volumes is embedded in the formulation, and there is no need to construct a dual mesh system. The discrete approximations follow the standard FE practice, the FEM data structure is retained, and the discrete equations are processed in elements loop.

3.2. Temporal discretization

Spatial discretization of the governing equations has been carried out in the previous sections. The resulted equations (21) and (22) represent a set of ordinary differential equations:

$$\begin{bmatrix}\mathbf{P}_{ww} & \mathbf{C}_{wn}\\ \mathbf{C}_{nw} & \mathbf{P}_{nn}\end{bmatrix}\begin{bmatrix}\dfrac{\partial \mathbf{p}_w}{\partial t}\\ \dfrac{\partial \mathbf{p}_n}{\partial t}\end{bmatrix}+\begin{bmatrix}\mathbf{f}_w^{\text{int}}\\ \mathbf{f}_w^{\text{int}}\end{bmatrix}+\begin{bmatrix}\mathbf{f}_w^{\text{ext}}\\ \mathbf{f}_n^{\text{ext}}\end{bmatrix}=0 \tag{31}$$

Temporal discretization of this system is performed by the fully implicit first order accurate finite difference scheme. It results in the following nonlinear equation:

$$\begin{bmatrix}\mathbf{R}_{p_w}\\ \mathbf{R}_{p_n}\end{bmatrix}_{n+1}=\begin{bmatrix}\mathbf{P}_{ww} & \mathbf{C}_{wn}\\ \mathbf{C}_{nw} & \mathbf{P}_{nn}\end{bmatrix}_{n+1}\begin{bmatrix}\mathbf{p}_w\\ \mathbf{p}_n\end{bmatrix}_{n+1}+\begin{bmatrix}\Delta t\ \mathbf{f}_w^{\text{int}}\\ \Delta t\ \mathbf{f}_n^{\text{int}}\end{bmatrix}_{n+1}$$
$$+\begin{bmatrix}\Delta t\ \mathbf{f}_w^{\text{ext}}\\ \Delta t\ \mathbf{f}_n^{\text{ext}}\end{bmatrix}_{n+1}-\begin{bmatrix}\mathbf{P}_{ww} & \mathbf{C}_{wn}\\ \mathbf{C}_{nw} & \mathbf{P}_{nn}\end{bmatrix}_{n+1}\begin{bmatrix}\mathbf{p}_w\\ \mathbf{p}_n\end{bmatrix}_n=0 \tag{32}$$

where $\Delta t=t_{n+1}-t_n$ is the time step increment, and the subscripts n and $n+1$ denote time steps.

3.3. Linearization and solution strategy

Linearization of the system is performed using the Newton-Raphson algorithm. Through expanding equation (32) with the first-order truncated Taylor series, the following linear approximation can be obtained:

$$\mathbf{J}_{n+1}^{i}\begin{bmatrix}\Delta\mathbf{p}_w\\ \Delta\mathbf{p}_n\end{bmatrix}_{n+1}^{i+1}=-\begin{bmatrix}\mathbf{R}_{p_w}\\ \mathbf{R}_{p_n}\end{bmatrix}_{n+1}^{i} \tag{33}$$

where the subscripts denote iterations, and $\mathbf{J}$ is the well-known Jacobian matrix. By finding the solution of the linearized system of equations (33) , that is the increment of the nodal degrees of freedom, the corresponding nodal unknowns are subsequently attained through the following incremental relation:

$$\begin{bmatrix}\mathbf{p}_w\\ \mathbf{p}_n\end{bmatrix}_{n+1}^{i+1}=\begin{bmatrix}\mathbf{p}_w\\ \mathbf{p}_n\end{bmatrix}_{n+1}^{i}+\begin{bmatrix}\Delta\mathbf{p}_w\\ \Delta\mathbf{p}_n\end{bmatrix}_{n+1}^{i+1} \tag{34}$$

This implies that the vector of the nodal unknowns is improved at each time step as the iterative algorithm proceeds. This iterative process continues until the residual vector, $\mathbf{R}$, vanishes within the given tolerance. The Jacobian matrix in the full Newton-Raphson algorithm is defined as $\partial \mathbf{R}^i_{n+1} / \partial \mathbf{X}^i_{n+1}$:

$$\mathbf{J}^i_{n+1} = \begin{bmatrix} \mathbf{P}_{ww} + \Delta t.\left(\bar{\mathbf{P}}_{ww}\right) & \mathbf{C}_{wn} + \Delta t.\bar{\mathbf{C}}_{wn} \\ \mathbf{C}_{nw} + \Delta t.\bar{\mathbf{C}}_{nw} & \mathbf{P}_{nn} + \Delta t.\left(\bar{\mathbf{P}}_{nn}\right) \end{bmatrix}^i_{n+1} \quad (35)$$

in which the partial derivatives are calculated as:

$$\bar{\mathbf{P}}_{ww} = \frac{\partial \mathbf{f}^{\text{int}}_w}{\partial \mathbf{p}_w} = -\int_{\Gamma_{\text{int}}} \mathbf{W}^T \left\{ \left(\rho_w \frac{k_{rw}\mathbf{K}}{\mu_w} \nabla \mathbf{N} \right)^T .\mathbf{n} \right\}^T d\Gamma + \int_{\Gamma_{\text{int}}} \mathbf{W}^T \left\{ \left(\rho_w \frac{\mathbf{K}}{\mu_w} \frac{\partial k_{rw}}{\partial n_w} n'_w p_w \nabla \mathbf{N} \right)^T .\mathbf{n} \right\}^T d\Gamma \quad (36)$$

$$\bar{\mathbf{P}}_{nn} = \frac{\partial \mathbf{f}^{\text{int}}_n}{\partial \mathbf{p}_n} = -\int_{\Gamma_{\text{int}}} \mathbf{W}^T \left\{ \left(\rho_n \frac{k_{rn}\mathbf{K}}{\mu_n} \nabla \mathbf{N} \right)^T .\mathbf{n} \right\}^T d\Gamma - \int_{\Gamma_{\text{int}}} \mathbf{W}^T \left\{ \left(\rho_n \frac{\mathbf{K}}{\mu_n} \frac{\partial k_{rn}}{\partial n_w} n'_w p_n \nabla \mathbf{N} \right)^T .\mathbf{n} \right\}^T d\Gamma \quad (37)$$

$$\bar{\mathbf{C}}_{wn} = \frac{\partial \mathbf{f}^{\text{int}}_w}{\partial \mathbf{p}_n} = -\int_{\Gamma_{\text{int}}} \mathbf{W}^T \left\{ \left(\rho_w \frac{\mathbf{K}}{\mu_w} \frac{\partial k_{rw}}{\partial n_w} n'_w p_w \nabla \mathbf{N} \right)^T .\mathbf{n} \right\}^T d\Gamma \quad (38)$$

$$\bar{\mathbf{C}}_{nw} = \frac{\partial \mathbf{f}^{\text{int}}_n}{\partial \mathbf{p}_w} = \int_{\Gamma_{\text{int}}} \mathbf{W}^T \left\{ \left(\rho_n \frac{\mathbf{K}}{\mu_n} \frac{\partial k_{rn}}{\partial n_w} n'_w p_n \nabla \mathbf{N} \right)^T .\mathbf{n} \right\}^T d\Gamma \quad (39)$$

4. Numerical example

To show the efficiency of the proposed algorithm, a quarter of a five-spot water-flooding problem with a central low permeability zone is considered (Fig. 2). The central core region has an absolute permeability $K = 1.5$ millidarcy and the surrounding region has $K = 1.5$ darcy. The low permeability zone forms a barrier that splits the fluid flow in two parts. The relative permeability of each phase in this example is expressed by:

$$k_{rw} = \left(\frac{n_w - n_{wres}}{n_{wsat} - n_{wres}} \right)^{(2+3\lambda)/\lambda} \quad (40)$$

$$k_{ro} = \left(1 - \frac{n_w - n_{wres}}{n_{wsat} - n_{wres}} \right)^2 \left(1 - \left[\frac{n_w - n_{wres}}{n_{wsat} - n_{wres}} \right]^{(2+\lambda)/\lambda} \right) \quad (41)$$

where n_{wsat} is the volume fraction of the water phase at zero suction, n_{wres} is the residual volume fraction of water at very high suction, λ is a fitting parameter related to the pore size distribution. The following relation is assumed between the volume fraction of water and the capillary pressure:

$$n_w = n_{wres} + \left(n_{wsat} - n_{wres} \right) \left[\frac{p_d}{p_c} \right]^{\lambda} \quad (42)$$

where p_d is the displacement pressure for the water phase. The reservoir is initially saturated with 28% of water and 72% of oil, and the initial pressure is equal to zero. Water is injected into the domain from the lower left well and with the rate of 1600 liters per day, while the mixture of oil and water is produced from the upper right well. The total pore pressure at the production well is equal to zero, so the following system of equations should be considered:

$$p = \frac{n_w}{n} p_w + (1 - \frac{n_w}{n}) p_o = 0. \quad (43)$$

$$p_c = p_o - p_w \quad (44)$$

These equations are iteratively coupled with the whole system to ensure the fulfillment of the above-mentioned restrictions at the production well. The other relevant material properties and model parameters for this simulation are listed in Table 1. The contour plot of water saturation distribution after 1000 days of injection and also the streamlines are shown Fig, 3. As it can be seen, due to the very low permeability of the central zone, water front does not penetrate this zone and prefers to go through the higher permeable region.

In a similar example we can make the central zone more permeable than its surrounding in 3 orders of magnitude, i.e. 1.5 darcy for the central zone and 1.5 millidarcy for the surrounding. Similar contour plot of water saturation distribution and the streamlines are shown in Fig.

for this problem with high permeability in the central zone. As it is seen, injected water has smoothly entered and passed the high permeability zone. Ae expected, water flow has more concentrated in the central high permeable zone.

Table 1. Material properties and model parameters

Rock porosity, %	$n = 0.208$
Oil viscosity, cP	$\mu_o = 13.$
Water viscosity, cP	$\mu_w = 0.97$
Oil density, ton/m^3	$\rho_0 = 0.85$
Water density, ton/m^3	$\rho_w = 1.$
Relative permeability fitting parameter	$\lambda = 0.8$
Displacement pressure for water, kPa	$p_d = 2.$
Water residual volume fraction, %	$n_{wres} = 0.045$

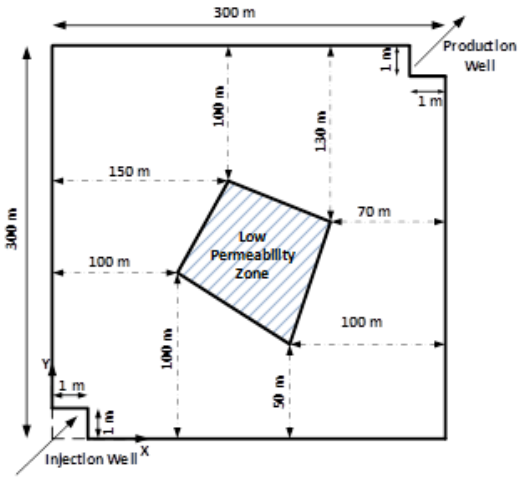

Fig. 2 Geometric configuration for the block heterogeneous problem.

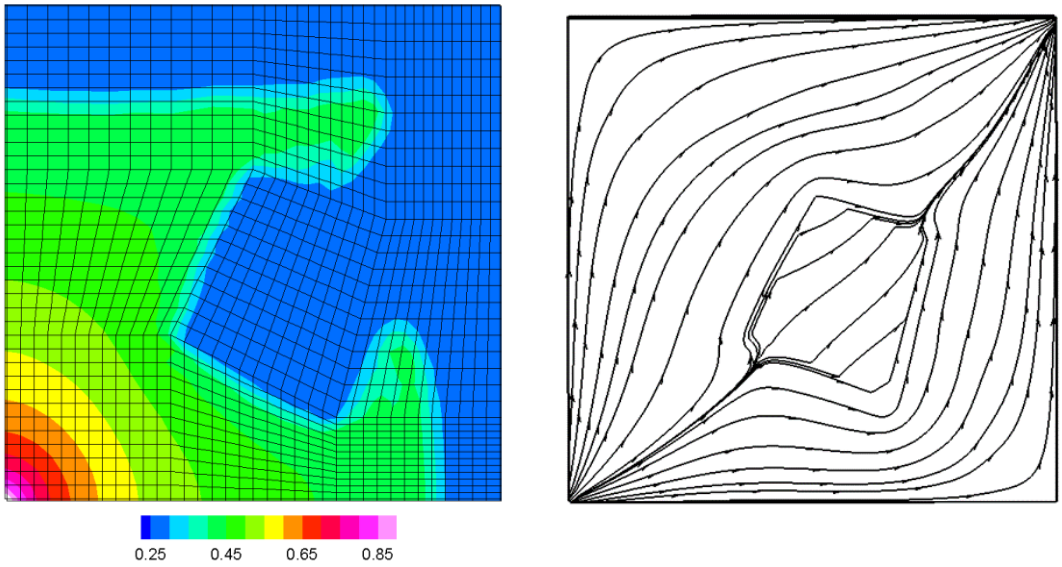

Fig. 3 Water saturation contours and streamlines for the block heterogeneous problem with low permeable central zone

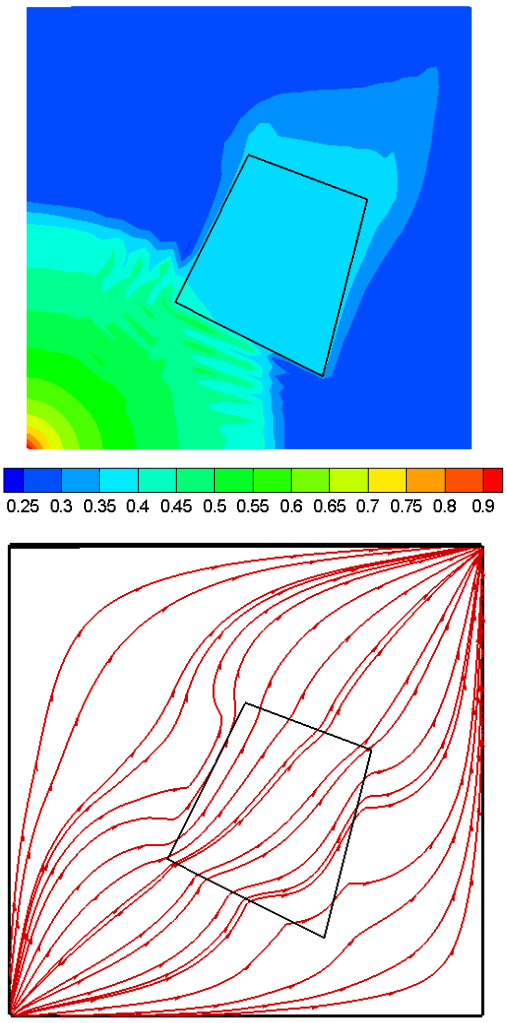

Fig. 4 Water saturation contours and streamlines for the block heterogeneous problem with high permeable central zone

5. Conclusions

In this paper, a CVFE solution of two-phase flow in geological porous media is presented. The discrete approximation follows the standard FE practice, and the FEM data structure is retained. The proposed solution satisfies the local and global conservation of mass, which has been demonstrated to be crucial in problems with distinct saturation shock front. A fully implicit first order accurate finite difference scheme has been employed for temporal discretization of the equations. A full Newton method with exact Jacobian is used to handle the nonlinearity of relative permeability terms in the system. A couple of five-spot water-flooding problem, with a central low and high permeability zone, has been chosen to illustrate the efficiency of the solution algorithm.

6. References

[1] Settari A, Aziz K (1975) Treatment of nonlinear terms in the numerical solution of partial differential equations for multiphase flow in porous media. International Journal of Multiphase Flow 1 (6):817-844.

[2] Chen Z, Huan G, Wang H (2006) Computer Simulation of Compositional Flow Using Unstructured Control Volume Finite Element Methods. Computing 78 (1):31-53.

[3] de Carvalho DKE, Willmersdorf RB, Lyra PRM (2007) A node-centred finite volume formulation for the solution of two-phase flows in non-homogeneous porous media. International Journal for Numerical Methods in Fluids 53 (8):1197-1219.

[4] Ghoreishian Amiri SA, Sadmejad SA, Ghasemzadeh H, Montazeri GH (2013) Application of control volume based finite element method for solving the black-oil fluid equations. Petroleum Science 10 (3):361-372.

[5] Wu YS, Forsyth PA (2001) On the selection of primary variables in numerical formulation for modeling multiphase flow in porous media. Journal of contaminant hydrology 48 (3-4):277-304.

[6] Ataie-Ashtiani B, Raeesi-Ardekani D (2010) Comparison of Numerical Formulations for Two-phase Flow in Porous Media. Geotechnical and Geological Engineering 28 (4):373-389.

[7] Taheri E, Sadmejad SA, Ghasemzadeh H (2017) Application of M3GM in a Petroleum Reservoir Simulation. Journal of Petroleum Science and Technology 7 (3):33-46.

[8] Sadmejad SA, Ghasemzadeh H, Taheri E Multiscale advanced features in modeling oil transport in porous media. In: 21st annual international conferences on mechanical engineering, Tehran, 2013.

[9] Pinder GF, Abriola LM (1986) On the simulation of nonaqueous phase organic compounds in the subsurface. Water Resources Research 22 (9S):109S-119S.

[10] Yin S, Dusseault MB, Rothenburg L (2009) Thermal reservoir modeling in petroleum geomechanics. International Journal for Numerical and Analytical Methods in Geomechanics 33 (4):449-485.

[11] Sadmejad SA, Ghasemzadeh H, Ghoreishian Amiri SA, Montazeri GH (2012) A control volume based finite element method for simulating incompressible two-phase flow in heterogeneous

porous media and its application to reservoir engineering. Petroleum Science 9 (4):485-497.

[12] Ghoreishian Amiri SA, Taheri E, Lavasan AA (2021) A hybrid finite element model for non-isothermal two-phase flow in deformable porous media. Computers & Geotechnics 135:104199.